Journal of Dental Sciences 20 (2025) 1406–1414

Available online at www.sciencedirect.com

ScienceDirect

journal homepage: www.e-jds.com

Original Article

Single-cell genomics reveals transcriptional heterogeneity and cellular crosstalk in salivary gland fibrosis

Dan Liang [a†], Wei Xu [b†], Yifan Wu [b], Qicheng Ye [b], Wanlin Xu [b**], Hao Lu [b*]

[a] *Department of Stomatology, Zhongshan Hospital, Fudan University, Shanghai, China*
[b] *Department of Oral and Maxillofacial-Head and Neck Oncology, Shanghai Ninth People's Hospital, College of Stomatology, Shanghai Jiao Tong University School of Medicine, National Clinical Research Center for Oral Disease, Shanghai Key Laboratory of Stomatology & Shanghai Research Institute of Stomatology, Shanghai, China*

Received 25 January 2025; Final revision received 15 February 2025
Available online 25 February 2025

KEYWORDS
Endothelial cell;
Salivary gland fibrosis;
Single-cell transcriptomics

Abstract *Background/purpose:* Salivary gland fibrosis (SGF) is a prevalent condition associated with various pathological states. However, a detailed understanding of the single-cell transcriptional profiles and cell–cell communication networks in this context remains elusive. Therefore, we aimed to unveil the gene expression profiles and intercellular communication patterns in SGF.
Materials and methods: We established fibrosis models of the submandibular gland (SMG) and generated a detailed single-cell transcriptomic atlas to investigate cellular heterogeneity and communication patterns. Utilizing CellChat, we dissected the intercellular dialogues within these fibrotic environments.
Results: The analysis distinguished fifteen distinct cellular clusters, highlighting significant heterogeneity among fibroblasts in fibrotic SMGs compared to their healthy counterparts. This heterogeneity was linked to TGF-β signaling, collagen fibril assembly, and extracellular matrix organization. CellChat analyses uncovered enhanced cell–cell interactions, notably between fibroblasts and endothelial cells (ECs) via the Gas6-Axl signaling axis. Additionally, our data indicated the activation of cell adhesion molecules and Rap1 pathways in ECs within the fibrotic SMG microenvironment.

* Corresponding author. Department of Oral and Maxillofacial-Head and Neck Oncology, Shanghai Ninth People's Hospital, College of Stomatology, Shanghai Jiao Tong University School of Medicine, No.639, Zhizaoju Road, Huangpu District, Shanghai 200011, China.
** Corresponding author. Department of Oral and Maxillofacial-Head and Neck Oncology, Shanghai Ninth People's Hospital, College of Stomatology, Shanghai Jiao Tong University School of Medicine, No.639, Zhizaoju Road, Huangpu District, Shanghai 200011, China.
E-mail addresses: xwl13661938595@126.com (W. Xu), tianbingxiaojiang@126.com (H. Lu).
† These two authors contributed equally to this work.

https://doi.org/10.1016/j.jds.2025.02.015

Conclusion: This study offers an in-depth single-cell resolution perspective on the cellular and molecular changes in SMG fibrosis, identifying new potential therapeutic targets for this condition.

Introduction

Fibrosis, a prevalent pathological state in salivary glands, arises from various triggers such as ductal obstruction, radiation exposure, aging, and autoimmune disorders like Sjögren's syndrome and immunoglobulin G4-related sialadenitis.[1—3] Characterized by fibroblast proliferation, enhanced collagen production, and extracellular matrix (ECM) deposition, SGF results in acinar cell atrophy and a decline in salivary function.[4] Despite extensive research on signaling pathways, including the TGF-β pathway, the heterogeneity among fibroblasts and their intercellular interactions with neighbor cell in SGF have not been thoroughly investigated.[5—7]

Fibroblasts, key players in ECM secretion, exhibit significant dynamism during fibrotic processes. Studies have shown that MCP-1-induced disruptions in endothelial tight junctions contribute to glandular fibrosis progression.[8] Identifying paracrine signals that facilitate communication between fibroblasts and surrounding cells is crucial for elucidating the mechanisms of SGF. Advances in single-cell RNA sequencing (scRNA-seq) and analytical algorithms have enabled the exploration of cellular heterogeneity and intercellular communication networks.[9,10] For instance, Li et al. identified new subpopulations of tissue-resident immune cells potentially involved in IgG4+ plasma cell generation in IgG4-related disease (IgG4-RD).[11] Rheinheimer et al. described ETV1+ cells, which may serve as acinar cell precursors in chronically irradiated parotid glands, using single-cell RNA sequencing.[12] However, a comprehensive single-cell atlas for SGF remains to be established.

In this study, we aimed to address these gaps by constructing a single-cell atlas that delineates the cellular composition, gene expression profiles, and intercellular communication patterns in a mouse duct ligation model of SMG fibrosis.

Materials and methods

Establishment of the animal model

This research was granted approval by the ethics committee of Shanghai Ninth People's Hospital, Shanghai Jiao Tong University School of Medicine. A mouse model for SGF was created by ligating the main excretory duct of the SMG, as previously detailed.[13] Eight-week-old female C57BL/6J mice, weighing between 18 and 20g, were acclimated to controlled environmental conditions and randomly assigned to either the fibrosis or control group. The fibrosis group underwent surgery to expose and ligate the main excretory ducts of the SMG under anesthesia. The control group was subjected to surgical incision only, without duct ligation. After a 14-day period post-ligation, the model was confirmed by ensuring the SMG weight was within 30—70 % of the average weight of the control group's SMG. Subsequently, the SMG tissues were collected for further experimental procedures.

Hematoxylin and eosin staining

Tissue samples were fixed in a 4 % paraformaldehyde solution overnight at 4 °C, followed by dehydration, paraffin embedding, and sectioning at 4-micron thickness onto glass slides. After xylene deparaffinization and graded alcohol rehydration, hematoxylin and eosin (H&E) staining was conducted according to standard protocols to assess histological changes.

Alcian blue periodic acid schiff stain

Alcian blue periodic acid schiff (AB-PAS) stain was utilized to evaluate salivary gland functionality during fibrosis. Tissue sections were treated with periodic acid and Schiff's reagent, resulting in a magenta coloration of the mucin area, indicative of mucin secretion.

Masson's trichrome staining

Masson's trichrome staining was performed to assess the extent of fibrosis, following standard procedures. Sections were sequentially stained with Weigert iron hematoxylin, acidic ethanol, Masson blue, biebrich scarlet, and weak acid solutions, resulting in hematoxylin-stained nuclei and Masson red-stained muscle fibers.

Immunohistochemical staining

Tissue sections were subjected to antigen retrieval via microwave heating and blocked with 10 % sheep serum for 1 h. Primary antibodies were applied overnight at 4 °C, followed by incubation with secondary antibodies for 30 min at 37 °C. DAB staining was used to visualize positive cells, and Image J software (NIH, Bethesda, MD, USA) was employed to quantify the stained area as a percentage of the total measured area.

Single-cell RNA sequencing and data preprocessing

The scRNA-seq was conducted by the laboratory staff at OE Biotech Co., Ltd. in Shanghai, China. The 10 × Genomics

Chromium Next GEM Single Cell 3′ Kit v3.1 was used for library preparation according to the user manual. SMG tissues were dissociated into single cells, and library construction and cDNA amplification were performed as per the protocol. High-throughput sequencing was carried out in PE-150 mode. Cells with over 200 expressed genes and a mitochondrial UMI rate below 40 % were included after quality control, with mitochondrial genes excluded from the expression matrix. The UMI count matrix was analyzed using the Seurat R package (version 4.0.0), and cells were visualized using a 2D Uniform Manifold Approximation and Projection (UMAP) algorithm. Clusters were annotated based on canonical marker genes, and GO and KEGG enrichment analyses were conducted to identify significantly enriched biological functions and pathways of differentially expressed genes (DEGs).

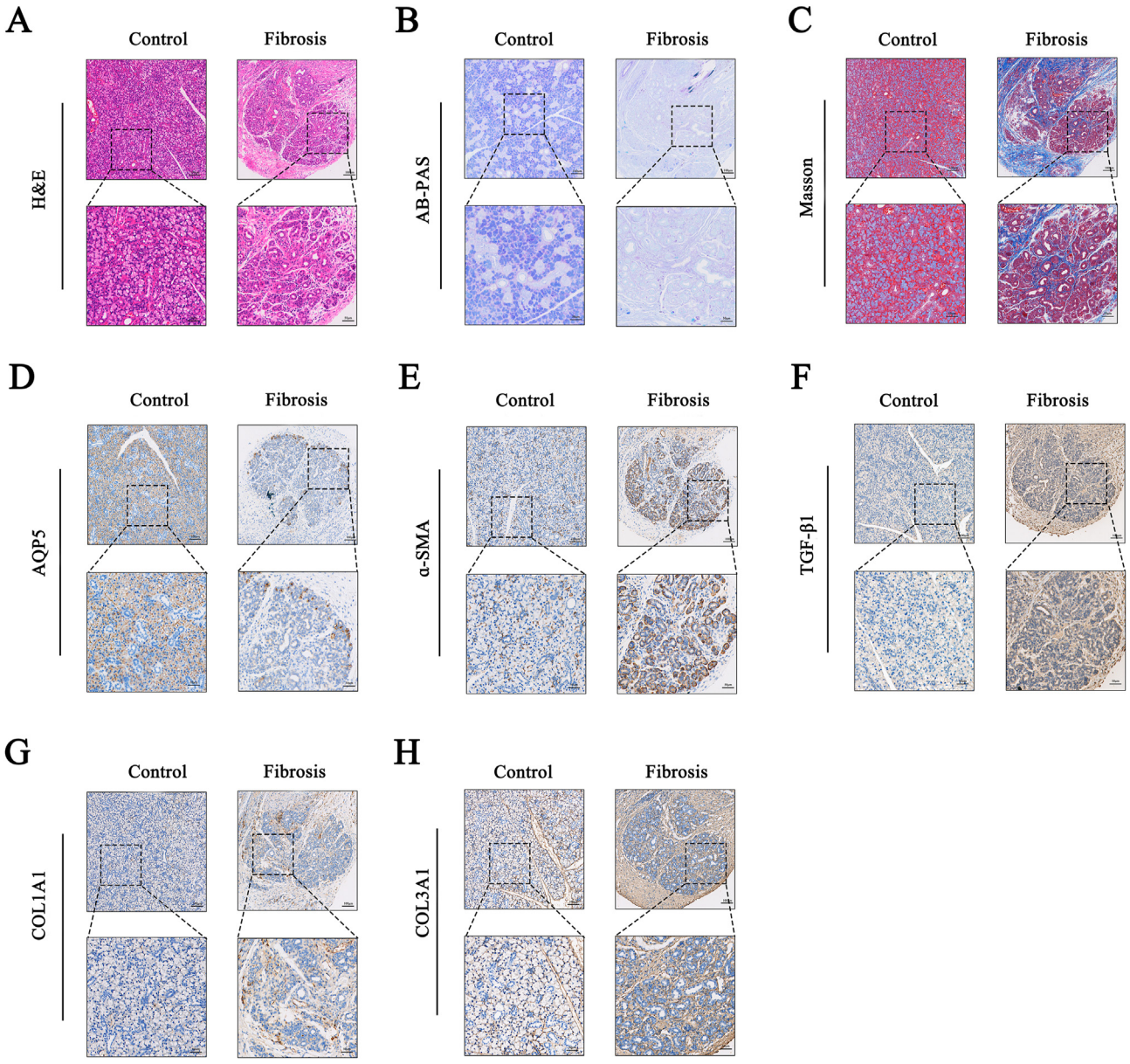

Figure 1 Evaluation of submandibular gland fibrosis after duct ligation. (A—C) The representative H&E, AB-PAS and Masson staining of SMG sections (bar = 100 μm under objective with × 10 amplification, bar = 50 μm under objective with × 20 amplification). (B) The representative AQP5, α-SMA and TGF-β1 staining of SMG sections (bar = 100 μm under objective with × 10 amplification, bar = 50 μm under objective with × 20 amplification). (C) The representative COL1A1 and COL3A1 staining of SMG sections (bar = 100 μm under objective with × 10 amplification, bar = 50 μm under objective with × 20 amplification). H&E, hematoxylin and eosin staining. AB-PAS, alcian blue periodic acid schiff. Masson, masson's trichrome staining. SMG, submandibular gland. AQP5, aquaporin-5. α-SMA, α-smooth muscle actin. TGF-β1, transforming growth factor beta 1. COL1A1, collagen type I alpha 1 chain. COL3A1, collagen type III alpha 1 chain.

Cell communication analysis

CellChat (version 1.1.3) was utilized to analyze cell–cell communication molecules, with ligand-receptor networks enriched based on the expression patterns across different clusters. The significance of ligand-receptor interactions (P-value <0.05) for each cell pair was determined based on the normalized cell matrix obtained through Seurat normalization.

Statistical analysis

Data are presented as mean ± standard error, with statistical significance set at P-value <0.05. Graphs were generated using GraphPad Prism 8 software (GraphPad Software, San Diego, CA, USA).

Results

Evaluation of SMG fibrosis in the duct ligation model

We initially assessed the SMG fibrosis model, which was induced by ligating the main excretory duct. Histological evaluation (H&E) staining revealed significant atrophy of acini and duct dilation in the duct-ligated group (Fig. 1A). AB-PAS staining indicated a reduction in mucin production after duct ligation (Fig. 1B). Masson's trichrome staining demonstrated an increase in collagen fiber deposition in the interlobular and intralobular spaces (Fig. 1C). Correspondingly, IHC staining showed a significant decline in the acinar marker AQP5 during the fibrosis (Fig. 1D). Meanwhile, the myofibroblast marker α-SMA and the recognized fibrotic biomarker TGF-β1 were highly enriched in the ligated group compared to controls (Fig. 1E and F). Similarly, the key fibrotic markers COL1A1 and COL3A1 were significantly upregulation post-ligation (Fig. 1G and H). These findings confirm the successful establishment of the SMG fibrosis model via the main excretory duct ligation.

Characterization of SMG single-cell atlas

To map the cellular architecture of fibrosis, we conducted scRNA-seq on healthy and fibrotic mouse SMG tissues. Post-quality control, a total of 15,796 single cells were processed for further analysis. As depicted in Fig. 2A and B, fifteen distinct cell clusters were identified based on genetic signatures and marker expression. These included acinar cells (Chia1+), intercalated duct cells (Dcpp2+), striated duct cells (Fxyd2+), myoepithelial cells (Krt14+), endothelial cells (Cdh5+), fibroblast stromal (Lum+), epithelial cell (Epcam+), schwann cell (Kcna1+), pericyte (Rgs4+), plasma cell (Sdc1+), and various immune populations such as T-cells (Cd3d+), B-cells (Cd19+), macrophages (C1qa+), dendritic

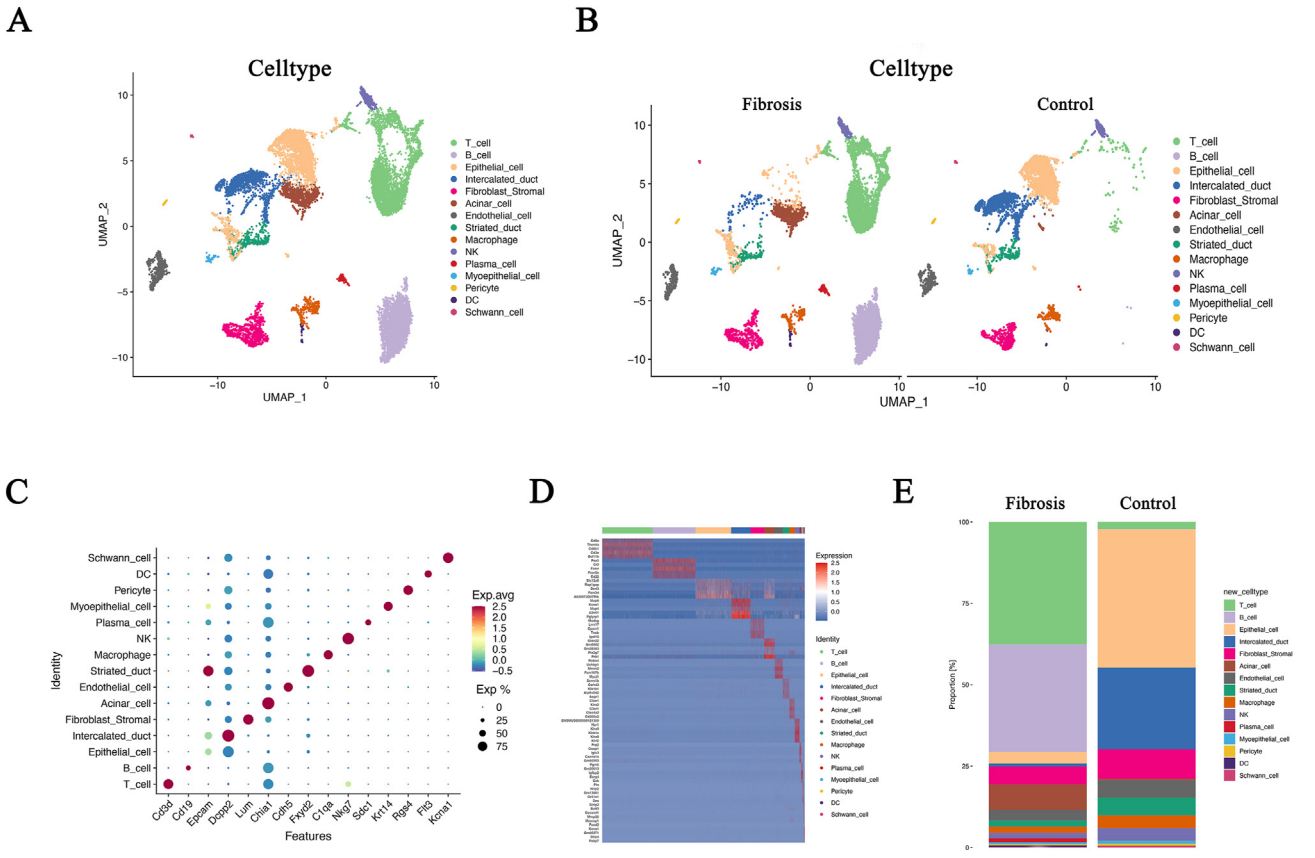

Figure 2 Single-cell RNA sequencing profiling of SMG fibrosis and control. (A) UMAP plot for 15 cell types from total tissues. (B) UMAP visualization grouped by SMG fibrosis and control. (C–D) The dot plot and heatmap showing the expression of marker genes of each cell type. (E) Relative percentage of cell subtypes across SMG fibrosis and control group. SMG, submandibular gland. UMAP, uniform manifold approximation and projection.

cells (Flt3+), and natural killer cells (Nkg7+) (Fig. 2C and D). Interestingly, fibrotic SMG exhibited decreased percentages of several cell types such as fibroblast stromal cells but increased T cell and B cell proportions (Fig. 2E). Notably, the primary cell types were consistent across groups, with variations in their relative abundances.

Comparative analysis of the heterogeneity of fibroblasts in SMG

Comparative analysis of fibroblast heterogeneity in SGF reveals distinct subpopulations with unique functional roles. Our study identified five distinct fibroblast subpopulations within SGF, characterized by specific gene expression patterns (Fig. 3A–C). Notably, Mfap4+ fibroblasts, implicated in elastic fiber formation and cell interactions, were prominent alongside Aif1l+ and Aqp5+ fibroblasts. Additionally, Prpmp5+ and Plekha6+ fibroblasts were identified, all of which are integral to fibroblast function. Interestingly, fibrotic SMG exhibited an increased presence of Aif1l+, Mfap4+, and Prpmp5+ fibroblasts, while Plekha6+ and Aqp5+ fibroblasts were less abundant (Fig. 3D and E). GO enrichment analysis, based on differentially expressed genes (DEGs), indicated heightened

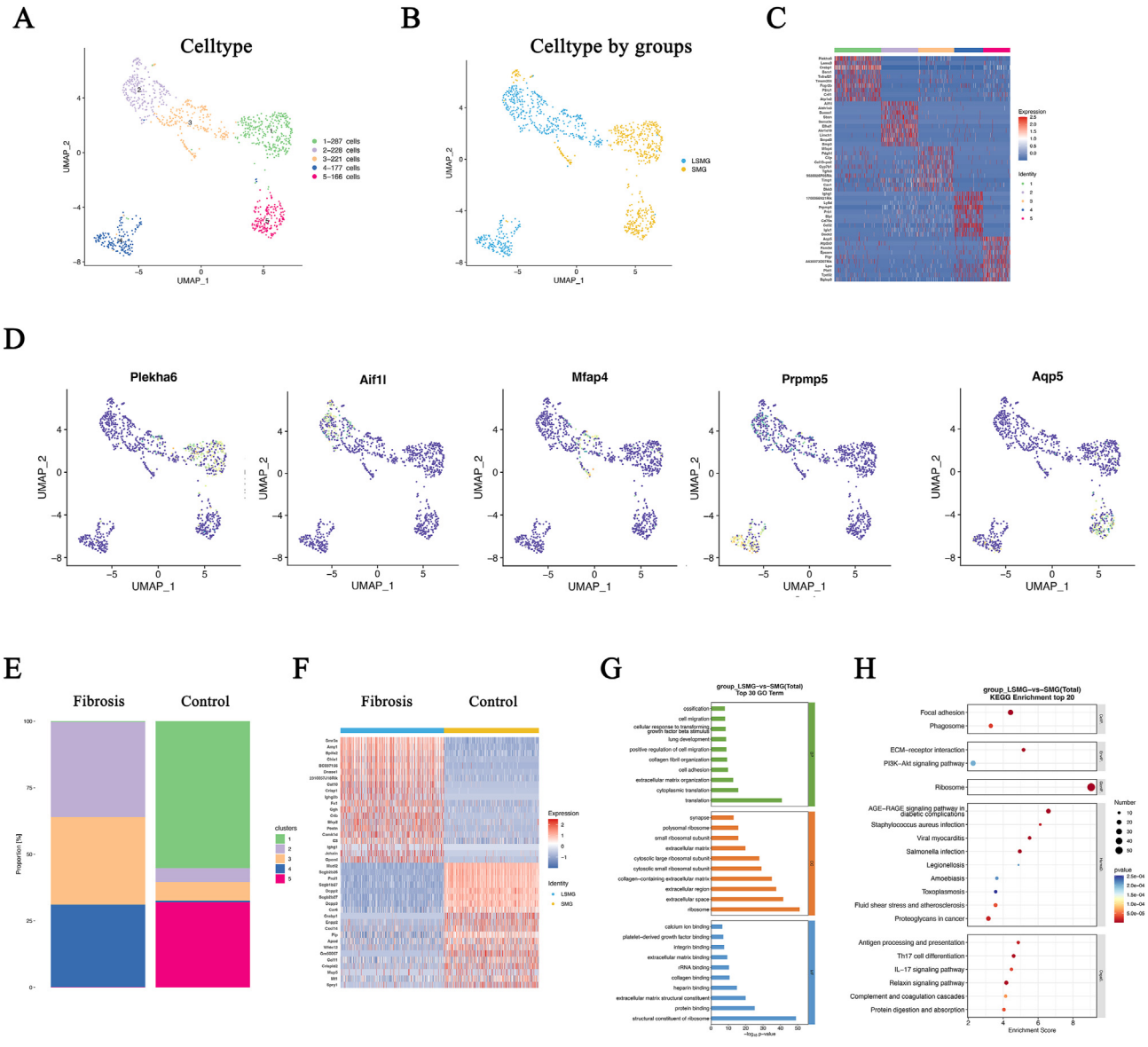

Figure 3 Heterogeneity of fibroblasts during the fibrosis of SMG. (A) UMAP plot view of heterogeneity of fibroblasts from total tissues. (B) UMAP plot view of heterogeneity of fibroblasts by SMG fibrosis and control. (C) The heatmap showing the expression of marker genes of each fibroblast cell type. (D) Expression levels of portion of specific cell markers on UMAP plots. (E) The fraction of fibroblast subclusters from SMG fibrosis and control. (F) The heatmap showing the different expressed genes in fibroblasts across SMG fibrosis and control group. (G) GO classification provides putative gene functions for fibroblasts in fibroblasts during the fibrosis of SMG. (H) KEGG pathway enrichment analysis showing the activated pathways in fibroblasts during the fibrosis of SMG. SMG, submandibular gland. UMAP, uniform manifold approximation and projection. GO, gene ontology. KEGG, the Kyoto Encyclopedia of Genes and Genomes.

fibroblast activity in fibrotic SMG, particularly in responses to TGF-β, collagen fibril organization, and ECM organization (Fig. 3F and G). KEGG analysis of our scRNA-seq data highlighted the ECM-receptor interaction pathway as a key regulator in fibrotic SMG (Fig. 3H).

Identification of cell–cell interaction in the fibrotic SMG

Investigating cell–cell interactions in fibrotic SMG, we observed an escalation in both the quantity and intensity of interactions compared to healthy SMG (Fig. 4A and B). This increase was over threefold in interaction numbers and over fourfold in interaction strength during fibrosis (Fig. 4C). A significant enhancement in interactions between fibroblasts and other cell types, notably endothelial cells (ECs), was observed (Fig. 4D). Ligand-receptor pair analysis identified Gas6-Axl as a pivotal interaction between fibroblasts and ECs in fibrotic SMG, with Gas6 expression in ECs markedly elevated (Fig. 4E).

Delineating specific ECs clusters occurred in the fibrosis of SMG

Focusing on the pivotal role of ECs in fibroblast function, we dissected EC subsets and noted significant heterogeneity among them (Fig. 5A–C). Fibrotic SMG showed an increased presence of Amy1+ and Cd8b1+ ECs, contrasting with a decrease in Prol1+, Mup5+, and Aspn + ECs (Fig. 5D and E).

Further GO and KEGG analyses revealed processes and pathways associated with cellular responses to the Rap1 signaling pathway and cell adhesion molecules, both of which are crucial in fibrosis progression (Fig. 5F–H).

Dysregulated intercellular communications in the fibrosis of SMG

Other than endothelial cells, we also focus on the dysregulated intercellular communications between the acinar cells, striated duct, intercalated duct, and myoepithelial cells during the fibrosis of SMG. As shown in Fig. 6A and B, both the quantity and intensity of interactions increased significantly in the fibrosis SMG compared to healthy SMG. This increase was over threefold in interaction numbers and over twofold in interaction strength during the progress of fibrosis (Fig. 6C). Many well-known signaling pathways have changed, such as the EGF-EGFR signaling pathway, which is significantly activated during the process of fibrosis (Fig. 6D).

Discussion

Despite substantial research on SGF, specific cell populations contributing to the disease remain poorly understood. In this study, we utilized scRNA-seq to construct a comprehensive gene expression atlas of SGF, identifying fifteen major cell types associated with fibrosis progression through UMAP clustering. Notably, we discovered that ECs

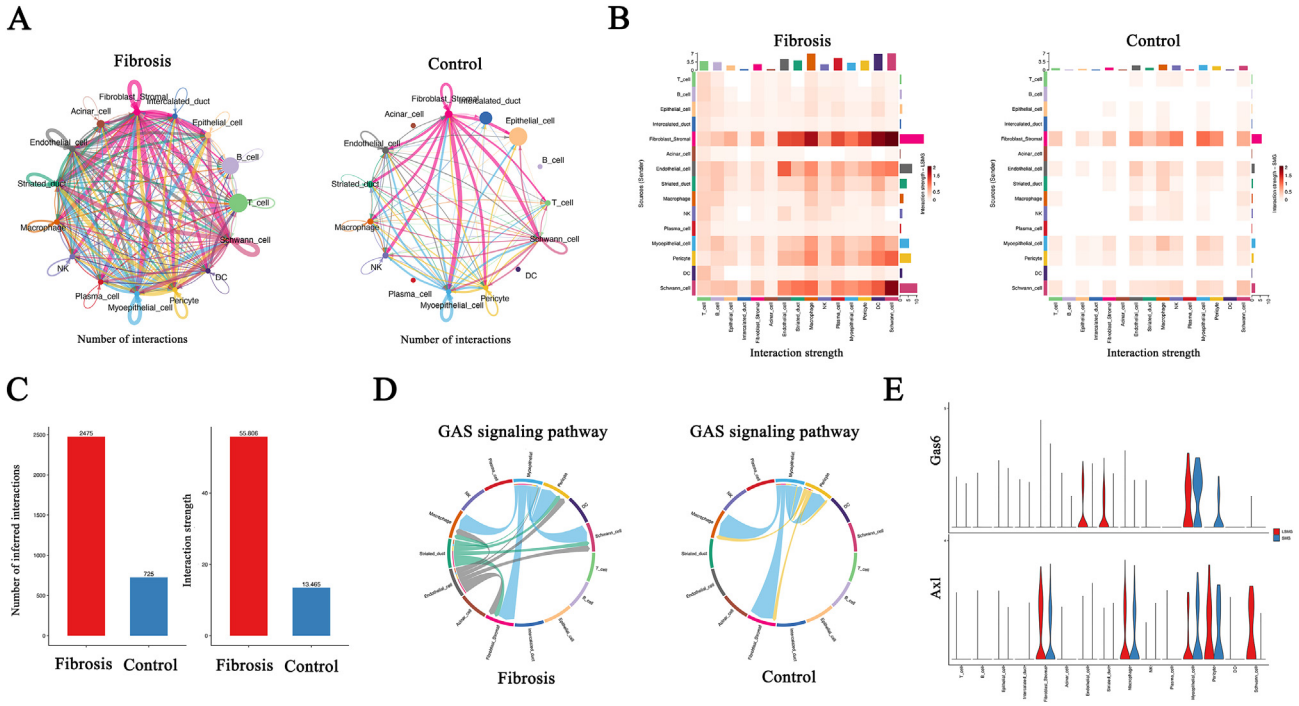

Figure 4 Dysregulated intercellular communications during the fibrosis of SMG. (A) The number of intercellular interactions among different cell types split by groups of SMG fibrosis and control. (B) The strength of intercellular interactions among different cell types split by groups of SMG fibrosis and control. (C) Number of ligand-receptor pairs and interaction strength in SMG fibrosis and control by CellChat. (D) The GAS signaling pathway among different cell types. (E) Relative mRNA level of Gas6 and Axl in different cell types. SMG, submandibular gland. GAS, growth arrest-specific protein. Axl, axl receptor tyrosine kinase.

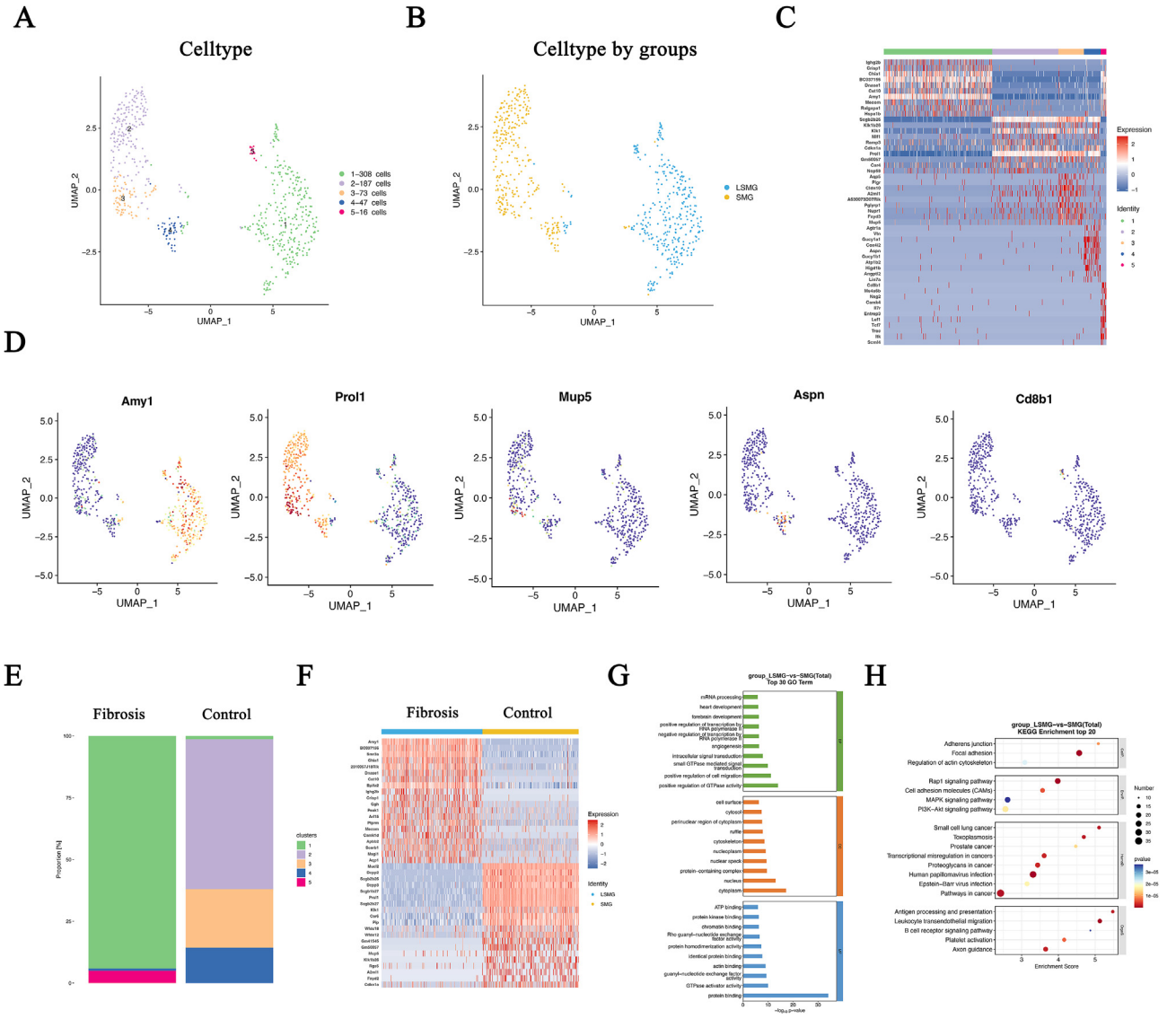

Figure 5 Heterogeneity of ECs during the fibrosis of SMG. (A) UMAP plot view of heterogeneity of ECs from total tissues. (B) UMAP plot view of heterogeneity of ECs by SMG fibrosis and control. (C) The heatmap showing the expression of marker genes of each cell type. (D) Expression levels of portion of specific cell markers on UMAP plots. (E) The fraction of EC subclusters from SMG fibrosis and control. (F) The heatmap showing the different expressed genes across SMG fibrosis and control group in ECs. (G) GO classification provides putative gene functions for fibroblasts in ECs during the fibrosis of SMG. (H) KEGG pathway enrichment analysis showing the activated pathways in ECs during the fibrosis of SMG. ECs, endothelial cells. SMG, submandibular gland. UMAP, uniform manifold approximation and projection. GO, gene ontology. KEGG, the Kyoto Encyclopedia of Genes and Genomes.

secreting Gas6 and binding to fibroblast Axl play a crucial role in fibroblast activation during SMG fibrosis. These findings offer novel insights into the mechanisms of cell—cell communication in fibrosis.

We established a mouse model with unilateral ligation of the main excretory duct of the SMG to induce fibrosis. Histological evaluations using H&E, AB-PAS, and Masson trichrome staining confirmed successful fibrosis induction, characterized by increased fibrosis, acinar cell atrophy, and reduced mucin secretion. Elevated expression of α-SMA, TGF-β1, COL1A1 and COL3A1 further validated the extent of fibrosis, which was consist with previous studies.[13,14]

Fibroblasts, critical for ECM secretion during fibrosis, exhibit heterogeneity across tissues. Previous study showed that Pdgfr+ and Gli1+ stromal fibroblasts are potentially contributed to glandular fibrosis.[15] Another study also revealed that Col15a1+ fibroblasts exhibited a distinct transcriptome in IgG4-RD.[16] Our results revealed an increase in Aif1l+, Mfap4+, and Prpmp5+ fibroblasts in fibrotic SMG, contributing to collagen fibril and ECM organization. MFAP4, a 36-kDa extracellular matrix glycoprotein, is implicated in organ fibrosis, elastic fiber formation, and cell interactions.[17] We also observed an enrichment in cell—cell communication, both in number and strength, during SMG fibrosis, indicating active signaling pathways. Recent studies have implicated endothelial cells in fibrosis.[18,19] He et al. showed that endothelial POFUT1 prevents liver fibrosis by repressing fibrinogen expression.[20]

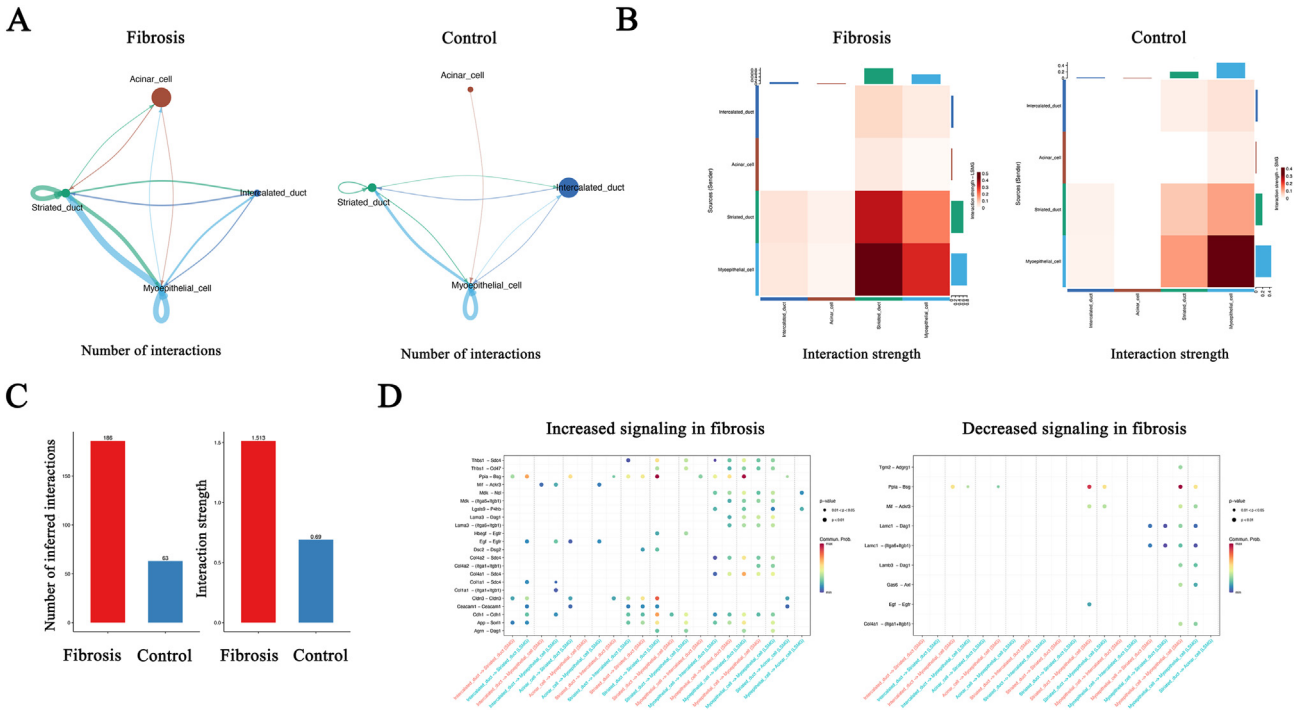

Figure 6 Dysregulated intercellular communications between the acinar cells, striated duct, intercalated duct, and myoepithelial cells during the fibrosis of SMG. (A) The number of intercellular interactions among different cell types split by groups of SMG fibrosis and control. (B) The strength of intercellular interactions among different cell types split by groups of SMG fibrosis and control. (C) Number of ligand-receptor pairs and interaction strength in SMG fibrosis and control by CellChat. (D) The increased and decreased signaling in fibrosis between the acinar cells, striated duct, intercalated duct, and myoepithelial cells. SMG, submandibular gland.

In our study, Gas6-Axl interaction was identified as a key communication pathway between fibroblasts and ECs in fibrotic SMG. The combination of Gas6 and Axl has been reported to increase α-SMA expression and promote liver fibrosis.[21] Additionally, the Gas6-Axl pathway is known to play a critical role in fibrogenesis via activation of hepatic stellate cells.[22] We further detected heterogeneity among ECs during SMG fibrosis, with increased Amy1+ and Cd8b1+ ECs associated with interleukin-1 and Rap1 signaling pathways. Similar findings have been observed in atrial tissue, where ECs are involved in atrial fibrillation through TXNDC5 and POSTN.[23] The activation of Rap1 in endothelial cells plays a significant role for fibrosis enhancements. Firstly, the activation of Rap1 can mediate the potent profibrotic cytokine TGF-b signaling pathway and the expression of fibrosis related genes, such as a-SMA and Cola1a.[24] Secondly, Rap1 activation in ECs can increase the expression of adhesion molecules, which make it easier for leukocytes to migrate into the tissue and release inflammatory mediators and cytokines.[8,25,26] Thirdly, ECs with Rap1 activation can secrete ECM components, which may directly promote the development of fibrosis.[27]

However, our study has limitations. The single-cell database is based on an animal model, and the results require validation in samples from patients with SGF. Furthermore, the intercellular communication between fibroblasts and ECs warrants further exploration in vitro.

In conclusion, our study provides the first description of fibroblast subtype heterogeneity and highlights the cross-talk between fibroblasts and ECs at a single-cell resolution in SGF. We also discovered a novel pattern of fibroblasts communication with ECs through the Gas-Axl pathway, offering a fresh perspective for understanding SGF.

Declaration of competing interest

The authors declare that they have no known competing financial interests or personal relationships that could have appeared to influence the work reported in this paper.

Acknowledgements

This work was supported by Fund of Department of Oral and Maxillofacial Surgery (202306), Fundamental research program funding of Ninth People's Hospital affiliated to Shanghai Jiao Tong university School of Medicine (JYZZ216), and the Biobank Project of Shanghai Ninth People's Hospital (YBKB202214).

References

1. Leehan KM, Pezant NP, Rasmussen A, et al. Minor salivary gland fibrosis in Sjögren's syndrome is elevated, associated with focus score and not solely a consequence of aging. *Clin Exp Rheumatol* 2018;36(Suppl 112):80–8.
2. Stone JH, Zen Y, Deshpande V. IgG4-related disease. *N Engl J Med* 2012;366:539–51.

3. Straub JM, New J, Hamilton CD, et al. Radiation-induced fibrosis: mechanisms and implications for therapy. *J Cancer Res Clin Oncol* 2015;141:1985—94.
4. Zhang Z, Li H, Wang G, et al. Thrombospondin-1 and prolyl 4-hydroxylase subunit alpha 3 as potential biomarkers of salivary gland fibrosis. *J Dent Sci* 2023;18:1243—50.
5. Chen Z, Chen X, Zhu B, et al. TGF-β1 triggers salivary hypofunction via attenuating protein secretion and AQP5 expression in human submandibular gland cells. *J Proteome Res* 2023;22:2803—13.
6. Li H, Cao Y, Zhao G, et al. ORAI2 is important for the development of early-stage postirradiation fibrosis in salivary glands. *Int J Radiat Oncol Biol Phys* 2024;24:03449.
7. Li H, Wang G, Hu M, et al. Specific inhibitor of Smad3 (SIS3) alleviated submandibular gland fibrosis and dysfunction after dominant duct ligation in mice. *J Dent Sci* 2023;18:865—71.
8. Mao XD, Min SN, Zhu MQ, et al. The role of endothelial barrier function in the fibrosis of salivary gland. *J Dent Res* 2023;102:82—92.
9. Kolodziejczyk AA, Kim JK, Svensson V, et al. The technology and biology of single-cell RNA sequencing. *Mol Cell* 2015;58:610—20.
10. Oyelakin A, Song EAC, Min S, et al. Transcriptomic and single-cell analysis of the murine parotid gland. *J Dent Res* 2019;98:1539—47.
11. Li Y, Wang Z, Han F, et al. Single-cell transcriptome analysis profiles cellular and molecular alterations in submandibular gland and blood in IgG4-related disease. *Ann Rheum Dis* 2023;82:1348—58.
12. Rheinheimer BA, Pasquale MC, Limesand KH, et al. Evaluating the transcriptional landscape and cell-cell communication networks in chronically irradiated parotid glands. *iScience* 2023;26:106660.
13. Wang B, Li Z, An W, et al. Duct ligation/de-ligation model: exploring mechanisms for salivary gland injury and regeneration. *Front Cell Dev Biol* 2024;12:1399934.
14. Yang Y, Zi Y, Conglin D, et al. The NF-κB pathway plays a vital role in rat salivary gland atrophy model. *Heliyon* 2023;9:e14288.
15. Altrieth AL, Okeefe KJ, Gellatly VA, et al. Identifying fibrogenic cells following salivary gland obstructive injury. *Front Cell Dev Biol* 2023;11:1190386.
16. Tanaka S, Yamamoto T, Iwata A, et al. Single-cell RNA sequencing of submandibular gland reveals collagen type XV-positive fibroblasts as a disease-characterizing cell population of IgG4-related disease. *Arthritis Res Ther* 2024;26:55.
17. Wozny MR, Nelea V, Siddiqui IFS, et al. Microfibril-associated glycoprotein 4 forms octamers that mediate interactions with elastogenic proteins and cells. *Nat Commun* 2024;15:4015.
18. Trogisch FA, Abouissa A, Keles M, et al. Endothelial cells drive organ fibrosis in mice by inducing expression of the transcription factor SOX9. *Sci Transl Med* 2024;16:4581.
19. Bian F, Lan YW, Zhao S, et al. Lung endothelial cells regulate pulmonary fibrosis through FOXF1/R-Ras signaling. *Nat Commun* 2023;14:2560.
20. He S, Luo Y, Ma W, et al. Endothelial POFUT1 controls injury-induced liver fibrosis by repressing fibrinogen synthesis. *J Hepatol* 2024;81:135—48.
21. Bai YM, Yang F, Luo P, et al. Single-cell transcriptomic dissection of the cellular and molecular events underlying the triclosan-induced liver fibrosis in mice. *Mil Med Res* 2023;10:7.
22. Bárcena C, Stefanovic M, Tutusaus A, et al. Gas6/Axl pathway is activated in chronic liver disease and its targeting reduces fibrosis via hepatic stellate cell inactivation. *J Hepatol* 2015;63:670—8.
23. An N, Yang F, Zhang G, et al. Single-cell RNA sequencing reveals the contribution of smooth muscle cells and endothelial cells to fibrosis in human atrial tissue with atrial fibrillation. *Mol Med* 2024;30:247.
24. Moon MY, Kim HJ, Kim MJ, et al. Rap 1 regulates hepatic stellate cell migration through the modulation of RhoA activity in response to TGF-β1. *Int J Mol Med* 2019;44:491—502.
25. Su W, Wynne J, Pinheiro EM, et al. Rap1 and its effector RIAM are required for lymphocyte trafficking. *Blood* 2015;126:2695—703.
26. Wilson CW, Ye W. Regulation of vascular endothelial junction stability and remodeling through Rap1-Rasip1 signaling. *Cell Adhes Migrat* 2014;8:76—83.
27. Lakshmikanthan S, Zheng X, Nishijima Y, et al. Rap 1 promotes endothelial mechanosensing complex formation, NO release and normal endothelial function. *EMBO Rep* 2015;16:628—37.